

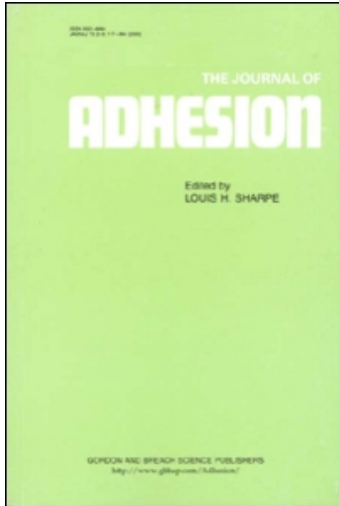
This article was downloaded by:

On: 22 January 2011

Access details: *Access Details: Free Access*

Publisher *Taylor & Francis*

Informa Ltd Registered in England and Wales Registered Number: 1072954 Registered office: Mortimer House, 37-41 Mortimer Street, London W1T 3JH, UK



The Journal of Adhesion

Publication details, including instructions for authors and subscription information:

<http://www.informaworld.com/smpp/title~content=t713453635>

Interfacial Characteristics of Sisal Fiber and Polymeric Matrices

Yan Li^{ab}; Yiu-Wing Mai^b

^a School of Aerospace Engineering and Applied Mechanics, Tongji University, Shanghai, China ^b

Centre for Advanced Materials Technology (CAMT), School of Aerospace, Mechanical and Mechatronic Engineering, University of Sydney, Sydney, Australia

To cite this Article Li, Yan and Mai, Yiu-Wing(2006) 'Interfacial Characteristics of Sisal Fiber and Polymeric Matrices', The Journal of Adhesion, 82: 5, 527 – 554

To link to this Article: DOI: 10.1080/00218460600713840

URL: <http://dx.doi.org/10.1080/00218460600713840>

PLEASE SCROLL DOWN FOR ARTICLE

Full terms and conditions of use: <http://www.informaworld.com/terms-and-conditions-of-access.pdf>

This article may be used for research, teaching and private study purposes. Any substantial or systematic reproduction, re-distribution, re-selling, loan or sub-licensing, systematic supply or distribution in any form to anyone is expressly forbidden.

The publisher does not give any warranty express or implied or make any representation that the contents will be complete or accurate or up to date. The accuracy of any instructions, formulae and drug doses should be independently verified with primary sources. The publisher shall not be liable for any loss, actions, claims, proceedings, demand or costs or damages whatsoever or howsoever caused arising directly or indirectly in connection with or arising out of the use of this material.

Interfacial Characteristics of Sisal Fiber and Polymeric Matrices

Yan Li

School of Aerospace Engineering and Applied Mechanics, Tongji University, Shanghai, China and Centre for Advanced Materials Technology (CAMT), School of Aerospace, Mechanical and Mechatronic Engineering, University of Sydney, Sydney, Australia

Yiu-Wing Mai

Centre for Advanced Materials Technology (CAMT), School of Aerospace, Mechanical and Mechatronic Engineering, University of Sydney, Sydney, Australia

Sisal-fiber-reinforced composites, as a class of eco-composites, have attracted much attention from materials scientists and engineers in recent years. In this article, the effects of fiber surface treatment on fiber tensile strength and fiber-matrix interface characteristics were determined by using tensile and single fiber pullout tests, respectively. The short beam shear test was also employed to evaluate the interlaminar shear strength of the composite laminates. Vinyl ester, epoxy, and high-density polyethylene (HDPE) were chosen as matrix materials. To enhance the interfacial strength, two kinds of fiber surface-treatment methods, namely, chemical bonding and oxidation, were used. The results obtained showed that different fiber surface-treatment methods produced different effects on the tensile strength of the sisal fiber and fiber-matrix interfacial bonding characteristics. Hence, valuable information on the interface design of sisal fiber-polymer matrix composites can be obtained from this study.

Keywords: Eco-composites; Fiber-matrix interface; Natural fiber; Shear strength; Sisal fiber

Received 4 December 2005; in final form 17 March 2006.

One of a collection of papers honoring Hugh R. Brown, who received *The Adhesion Society Award for Excellence in Adhesion Science, Sponsored by 3M*, in February 2006.

Address correspondence to Yiu-Wing Mai, Centre for Advanced Materials Technology (CAMT), School of Aerospace, Mechanical and Mechatronic Engineering J07, University of Sydney, NSW 2006, Australia. E-mail: mai@aeromech.usyd.edu.au

Present address of Yan Li is School of Aerospace Engineering and Applied Mechanics, Tongji University, Shanghai 200092, China.

1. INTRODUCTION

Natural fibers have received much attention from materials scientists and engineers in the past decades because they are inexpensive, lightweight, and biodegradable [1–3]. Several books have also been recently published that give comprehensive reviews of these very attractive materials [4–6]. The ability of natural fibers to replace current fibers in composite components could result in lower cost, lighter structures in addition to alleviating some of the increasing energy and resource crises. Using natural fibers as reinforcements in polymer composites opens up new applications for these agricultural by-products. Commercially important natural fibers are wood, bamboo, jute, sisal, kenaf, flax, ramie, coir, and hemp.

Sisal fiber is one of the strongest of all plant fibers. It is a hard natural fiber, which is obtained from the leaves of an annually harvested plant, called *Agave sisilana*. It is inexpensive, has a low-density, high specific strength and elastic modulus, is easily available and environment friendly, and can be recycled. Traditionally, sisal fiber is used to make ropes, mats, carpets, fishing nets, and fancy articles such as purses, wall hangings, table mats, etc. [7]. Usage of sisal fiber as a reinforcement in composites is driven by economic and ecological considerations. Some applications have been fulfilled, such as roofing [8], building materials [9], and automotive parts in recent years [10–12].

A sisal fiber is actually a bundle of hollow microfibers, and Figure 1 shows the cross-section of a single sisal fiber. The cell walls of microfibers are reinforced with spirally oriented cellulose in a hemi-cellulose and lignin matrix. The cell wall has a composite structure of lingocellulosic material reinforced by helical micro fibrillar bands of cellulose. The external surface of the cell wall is a layer of lignaceous material and waxy substances, which bond the cell to its adjacent neighbors. Hence, this surface will not form a strong bond with a polymer matrix. Furthermore, cellulose is a hydrophilic glucan polymer consisting of a linear chain of 1,4- β -bonded anhydroglucose units [13]. This large amount of hydroxyl groups gives sisal fiber hydrophilic properties, which leads to very poor interfacial adhesion between sisal fiber and the hydrophobic matrix and very poor moisture absorption resistance.

It is well known that the mechanical performance of a fiber-reinforced composite depends basically on three factors: (1) fiber strength and modulus, (2) matrix strength and chemical stability, and (3) effectiveness of interface bonding between matrix and fiber to enable stress transfer. A well-bonded interface is essential for effective stress transfer from matrix to fiber [14–16]. Although sisal fiber has recently

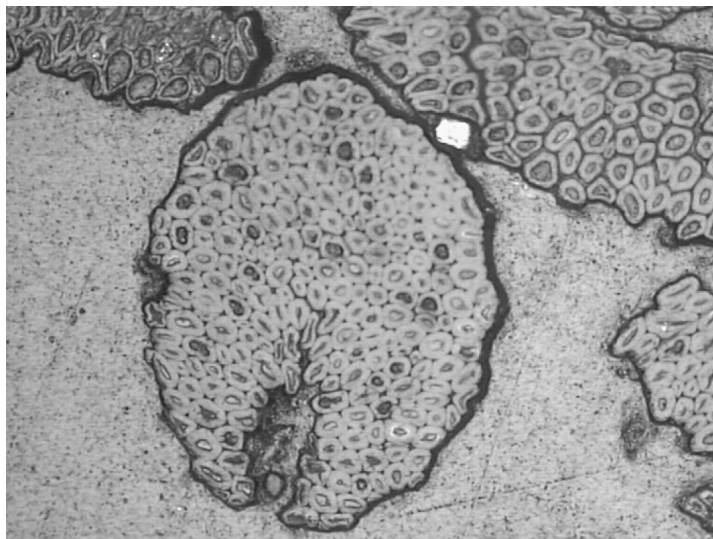


FIGURE 1 Cross-section of a single sisal fiber.

attracted great attention for the fabrication of sisal fiber composites, the poor interface between sisal fiber and polymer matrix, caused by the relatively few reactive groups of sisal and the hydrophilic nature of cellulose, has severely limited the application of sisal fiber as a reinforcement in composites [13]. Much effort has been devoted to the modification of the interface between natural fiber and polymer matrices [17–21]. However, the nature of the interface between sisal fiber and matrices has not been much studied, nor have the interfacial properties been quantitatively evaluated using single-fiber pullout [22,23] and other tests [16]. Most previous work was focused on the effects of modified sisal fiber–matrix interfaces on the mechanical properties of bulk composites, such as tensile, flexural, and impact strength, and so forth (see Rong et al. [24]). Detailed studies of interfacial shear strength (IFSS) and bonding mechanisms of the interface have been few to date (see Sydenstricker, Mochnaz, and Amico [25]).

For this article, the microstructure and properties of single sisal fibers were studied by using scanning electron microscopy (SEM) and mechanical tests to evaluate the interfacial properties of the composites. Different fiber surface treatments were used to improve the interfacial properties, and their effects on microstructure and failure mechanisms are discussed. A single-fiber pullout test was used to determine the interfacial bonding properties between sisal fibers

(treated and untreated) and several polymeric matrices [vinyl ester, epoxy, and high-density polyethylene (HDPE)]. Interfacial bonding mechanisms can be understood better by setting up different interfacial bonding levels using different matrices (which vary from thermosets to thermoplastics, polar to nonpolar, and low modulus to high modulus). Comparisons of single-fiber pullout interfacial properties were made, and the bonding mechanisms of interfaces were studied with SEM. Finally, a short-beam shear test was also conducted to evaluate the effect of fiber surface treatment on the interfacial properties of sisal textile composites.

2. MATERIALS AND FIBER SURFACE TREATMENT

2.1. Materials

Sisal fibers were provided by Kinnears Pty Ltd. Footscray, Australia, and their basic properties are listed in Table 1. Sisal textile used for making composites was obtained from Guangxi Province, China. This was plain woven and had identical properties in the orthotropic directions.

Vinyl ester resin (HETRON FR 992) was obtained from Ashland Chemical (Dublin, OH, USA) Pty. Ltd. The hardener was methyl ethyl ketone peroxide. Bisphenol (BPF) epoxy resin (EPON[®] 862) was provided by Shell Chemical Company, Harris County, TX, USA. The curing agent was 2-ethyl, 4 methyl imidazole. The HDPE was supplied by Hoechst (Australia) Ltd. Both vinyl ester resin and epoxy resin were cured at ambient temperature. Table 2 shows some properties of the polymers used in this study.

2.2. Fiber Surface Treatment Methods

2.2.1. Chemical Coupling

3-Aminopropyltriethoxy silane (silane 1) and gamma-methacryloxypropyltrimethoxy silane (silane 2) were used as coupling agents to

TABLE 1 Basic Properties of Sisal Fiber

Fiber diameter (μm)	Water content (%)	Tensile strength (MPa)	Tensile modulus (GPa)	Elongation at break (%)
100–300	9.8	100–700	25–50	3–6

TABLE 2 Mechanical and Physical Properties of Vinyl Ester, Epoxy, and HDPE

Property	Vinyl ester ^a	Epoxy ^b	HDPE ^c
Tensile strength (MPa)	35.20	59.90	26
Tensile modulus (GPa)	2.20	3.03	1.1
Elongation at break (%)	5.00	2.90	—
Flexural strength (MPa)	89.57	116.58	—
Flexural modulus (GPa)	2.58	3.23	—
Density (g/cm ³)	—	1.22	0.96

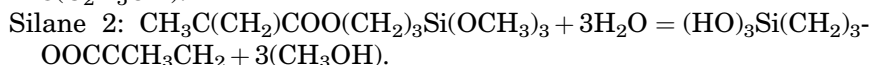
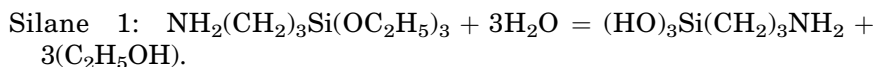
^aData obtained from Ashland Chemical Pty. Ltd.

^bData obtained from Shell Chemical Company.

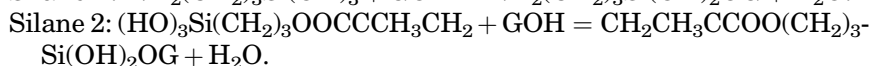
^cData obtained from Hoechst Australia Limited.

modify the surface of sisal fiber. They were diluted to 6% concentration in acetone before use. The sisal fibers were immersed in the silane solution for 24 h and then cleaned by acetone and dried in the oven at 60°C for 4 h to remove any excessive solvent. The chemical formulae of the silanes are silane 1, 3-aminopropyltriethoxy silane, H₂N(CH₂)₃Si(OC₂H₅)₃; and silane 2, gamma-methacryloxypropyltrimethoxy silane, CH₃C(CH₂)COO(CH₂)₃Si(OCH₃)₃.

In the presence of moisture, silane 1 and silane 2 react with water to form silanol and alcohol:



Then, silanol reacts with the hydroxyl groups attached to the glucose units, G, of the cellulose molecules in the fiber cell wall, thereby bonding itself to the cell wall and further rejecting water:



When combined with the matrix resin, other functional groups of the silane molecule, such as NH₂ and C = C groups, would react with the resin if it also contains suitable groups. Thus, chemical reactions occur among the sisal fiber, the matrix, and the coupling agent. Interfacial properties are improved by the resultant chemical bonding.

2.2.2. Oxidisation

Permanganate (KMnO_4) and dicumyl peroxide (DCP) were selected as oxidants to treat the fiber surface. Sisal fibers were immersed in a 0.055% permanganate acetone solution [21] for 2 min, cleaned with acetone, and dried at 60°C for 4 h to remove excessive solvent. For DCP treatment, the sisal fibers were immersed in a DCP acetone solution (6% concentration) for 1.5 h and washed with acetone. Drying was performed as for the permanganate treatment. Note that all fibers were heated in an oven at 120°C to remove the moisture before treatment, and all treated fibers were stored in sealed plastic bags before being used. It should be noted that the chemical reactions these two chemical agents might induce under certain conditions (such as with HDPE) were intentionally avoided so as to ensure that only physical bonding would occur.

2.3. Experimental Work

2.3.1. Single-Fiber Tensile Test

Single-fiber tensile tests were conducted according to ASTM D3379-75 to determine the tensile strength of treated and untreated sisal fibers using an Instron 5576 testing machine (Instron, Canton, MA, USA). A single fiber was selected and cut to 30 mm in length. Both ends of the sisal fiber were glued to the paper frame as shown in Figure 2.

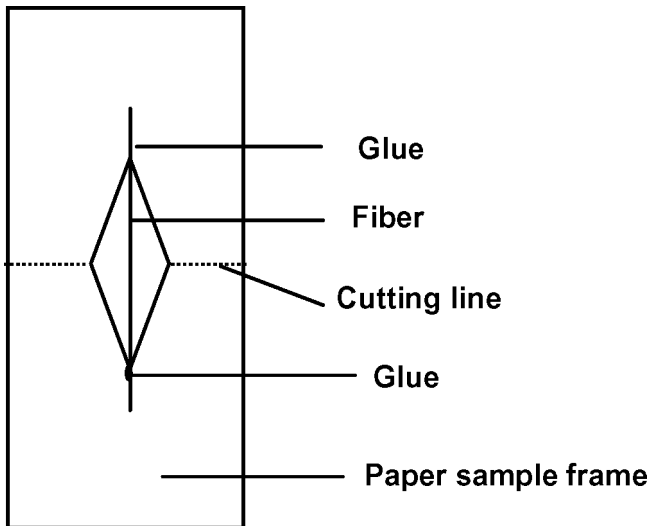


FIGURE 2 Sample preparation for single-fiber tensile tests.

The diameter of the sisal fiber was measured by an optical microscope before the test. The gauge length was controlled by the frame. After securing the specimen in the grips, the two sides of the paper frame were cut along the cutting line (Figure 2), and the fiber was then loaded until it failed in tension. The gauge length was 20 mm and the cross-head speed was 1 mm/min. The load-displacement curves were obtained.

2.3.2. Single-Fiber Pullout Test

The single-fiber pullout test is the most effective and convenient method to determine the fiber–matrix interfacial properties [22,23] and was used in this work despite some concerns about the nature of the singularity at the interface end [26]. The procedure for specimen preparation was different for thermoset (vinyl ester and epoxy) and thermoplastic (HDPE) matrices, which are described later.

Vinyl-ester and epoxy resins. First, a drop of the matrix resin was applied on a glass slide. The diameter of the matrix block was large enough (2 mm, about 10 fiber diameters) to avoid any boundary effect. Then one end of a sisal fiber was inserted into the middle of the drop. After the resin was cured, the glass slide was bonded to the paper frame and the free end of the fiber was glued to the other half of the frame as shown in Figure 3. The embedded fiber length was controlled by the inserted length of the sisal fiber into the matrix block and measured by an optical microscope before the fiber pullout test.

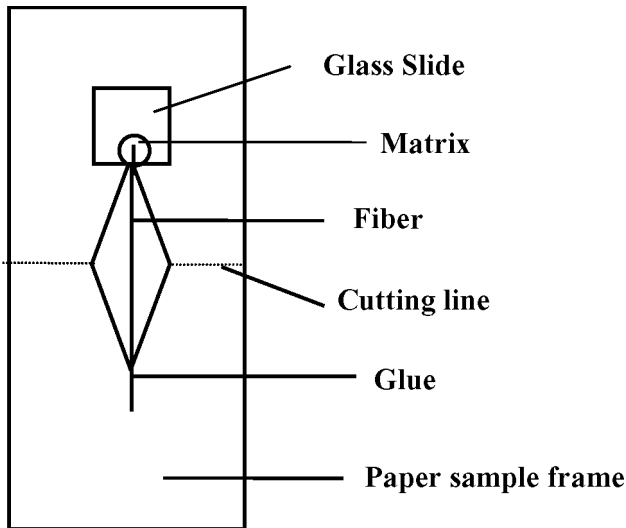


FIGURE 3 Schematic of specimen geometry of single-fiber pullout test.

HDPE resin. A polyamide film was folded and a machined slot introduced. The embedded fiber length was controlled by the width of the slot (Figure 4). Then, the film was unfolded, several sisal fibers were glued onto the film, and the film was folded again. Hence, the sisal fibers were protected between the films except for the slot, which would be exposed. The film and exposed fibers were embedded in the HDPE matrix and hot pressed at 180°C for 10 min. After cooling, excessive matrix material was removed and then attached to the paper frame described for the vinyl ester resin in Figure 3.

An Instron 5576 testing machine was used and the load-displacement curves were obtained during single-fiber pullout tests. After securing the specimen in the grips, the two sides of the paper frame were cut along the cutting line (Figure 3), and the fiber was loaded until it was pulled out from the matrix. The gauge length was 10 mm, and the cross-head speed 1 mm/min.

2.3.3. Short Beam Shear (SBS) Test

Both treated and untreated sisal textiles were used. Silane 2 and permanganate were chosen to treat the fiber surfaces. Two thermoset resins, vinyl ester and epoxy, were used as matrices for the sisal textile composite laminates made by resin transfer molding (RTM).

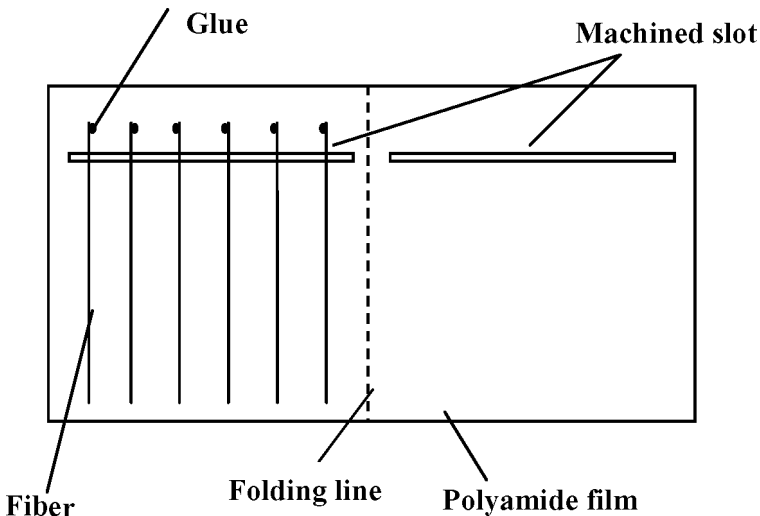


FIGURE 4 Schematic of sample preparation for sisal/HDPE single-fiber pullout test.

Specimens were cut from these laminates with nominal dimensions $24 \times 7 \times 3 \text{ mm}^3$, and the fiber volume fraction was $\sim 32\%$.

The SBS test was conducted in accordance with ASTM D-2344. The span length-to-depth ratio was 5, and the cross-head speed was 1.3 mm/min. At least 10 specimens were tested for each group. The tested specimens were examined to ensure that interlaminar shear failure rather than transverse damage was predominant.

3. RESULTS AND DISCUSSION

3.1. Properties of Sisal Fibers

3.1.1. Distribution of Tensile Strength and Diameter of Sisal Fibers

Distributions of untreated sisal fiber diameter and tensile strength, and the relationship between these two properties, are shown in Figures 5–7, respectively. It is well established that the structure and properties of sisal fibers are nonuniform, depending on which part of the leaf they were obtained from and which country of origin [27]. In Figure 5, the diameter of the sisal fibers varies from 100 to 300 μm , and almost 40% of the fibers have a diameter $\sim 200 \mu\text{m}$. The tensile strength of the sisal fibers varies between 50 and 900 MPa (see Figure 6). Almost 70% of the fibers have a tensile strength in the

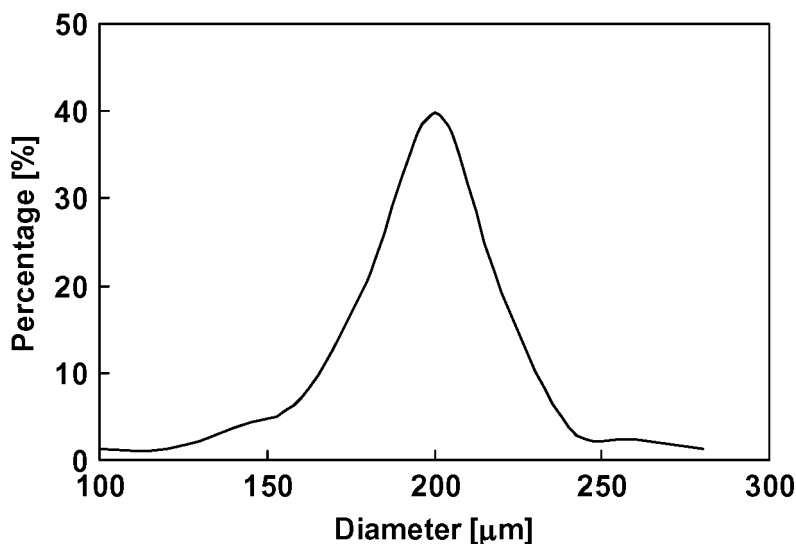


FIGURE 5 Distribution of sisal fiber diameter.

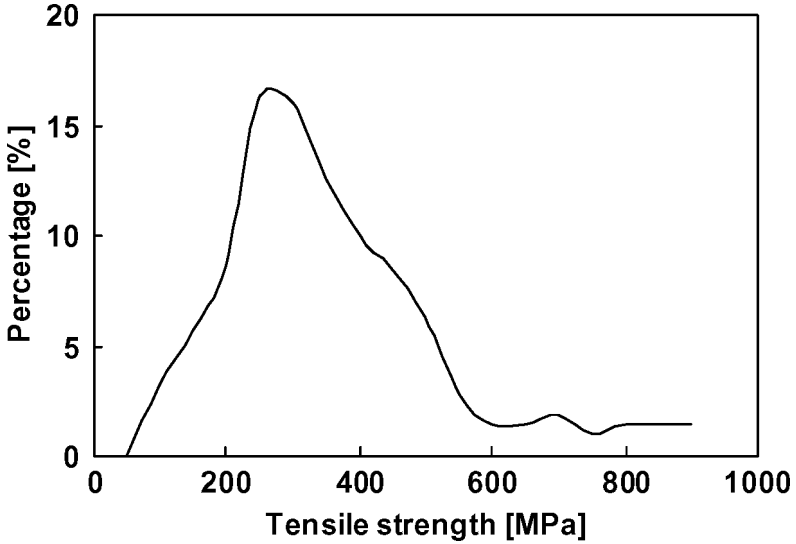


FIGURE 6 Distribution of sisal fiber tensile strength.

range 200 to 400 MPa. Figure 7 shows the correlation between fiber diameter and tensile strength. Larger fibers, as expected, have lower tensile strengths because they contain more defects.

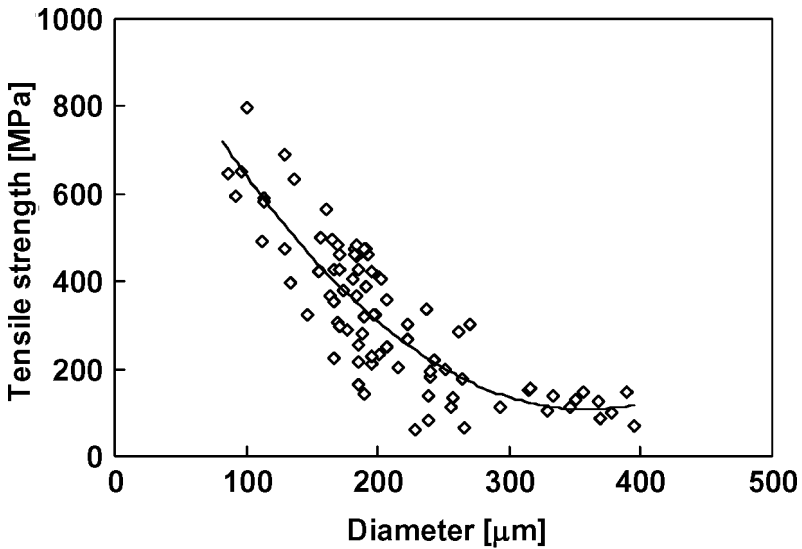


FIGURE 7 Distribution of sisal fiber tensile strength *versus* diameter.

3.1.2. Effect of Fiber Surface Treatment on Fiber Tensile Strength

Figure 8 shows a load-displacement curve obtained from a single sisal fiber tensile test. The tensile failure of sisal fiber is brittle. No plastic deformation was found before fiber breakage. All the load-extension curves for the sisal fiber tensile tests are linear.

The Weibull distribution has been widely used to describe the strength of brittle materials [28,29]. In this study, the Weibull shape and scale parameters are used to study the effect of fiber surface treatment on fiber strength. From the two-parameter Weibull model, the cumulative failure probability is given by

$$P = 1 - \exp \left\{ - \left[\frac{\sigma}{\sigma_0(s)} \right]^m \right\}, \quad (1)$$

where σ is applied stress, m is Weibull shape parameter, and $\sigma_0(s)$ is local scale parameter with a gauge length, s . The cumulative failure probability, P_i , under a particular stress is

$$P_i = \frac{(n_i - 0.5)}{n}, \quad (2)$$

where n_i is number of fibers fractured at or below an applied stress level and n is total number of fibers tested. In practice, a plot of $\ln[-\ln(1 - P)]$ versus $\ln(\sigma)$ is often used for a given specimen length

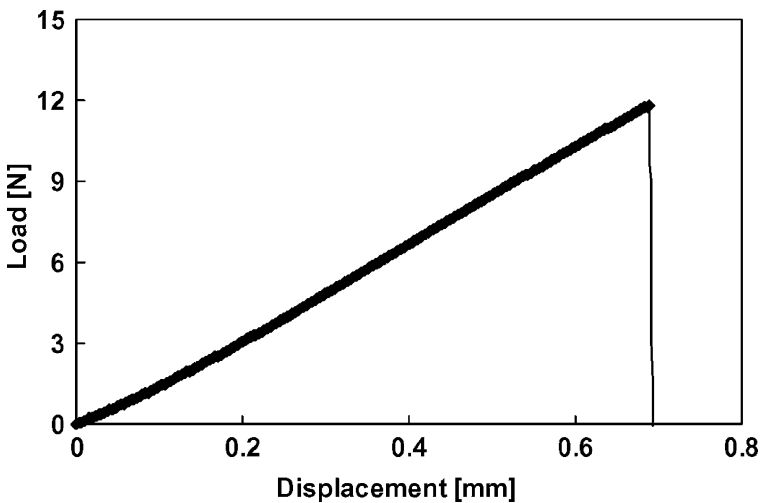


FIGURE 8 Typical load-extension curve during a single-fiber tensile test.

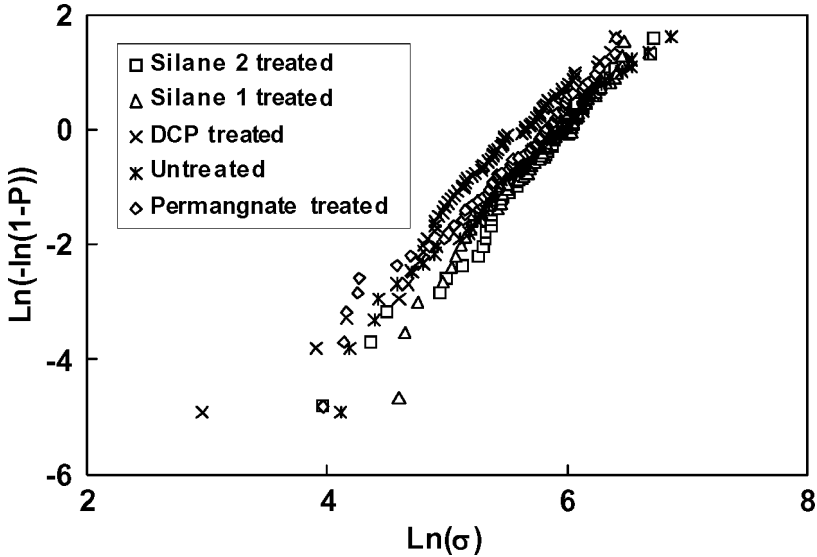


FIGURE 9 Weibull distribution of treated and untreated sisal fibers.

to determine the Weibull shape parameter, m , and scale parameter, $\sigma_0(s)$. Figure 9 shows plots of $\ln[-\ln(1-P)]$ versus $\ln(\sigma)$ for treated and untreated sisal fibers, which are in close agreement with Weibull's equation. The Weibull parameters, m and $\sigma_0(s)$, are calculated from Figure 9 and listed in Table 3. Variable m is a measure of the variability of fiber strength; a large value of m means small scatter and *vice versa*. Variable $\sigma_0(s)$ is a normalizing stress for a survival probability of 0.37.

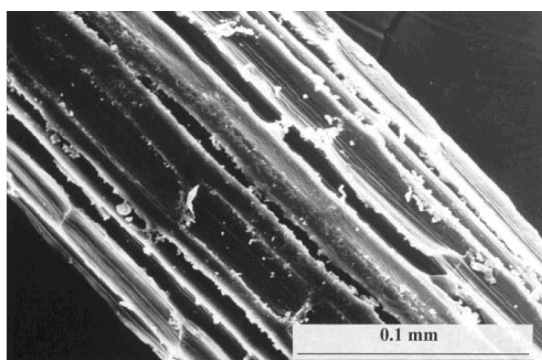
The results show that both permanganate and DCP treatments have smaller values of the Weibull shape parameter compared with

TABLE 3 Tensile Properties of Treated and Untreated Sisal Fibers

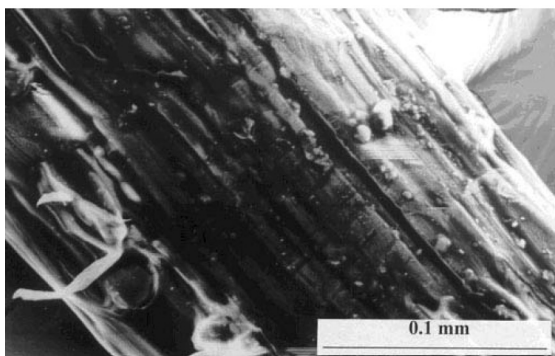
Fiber	Weibull shape parameter (m)	Weibull scale parameter $\sigma_0(s)$ (MPa)	Average tensile strength (MPa)
Untreated	2.44	380.93	338.62
KMnO ₄	2.14	333.34	292.58
DCP	2.12	283.03	249.43
Silane 1	2.54	391.39	346.95
Silane 2	2.46	390.21	345.59

the as-received and the two silane-treated sisal fibers. It is thought that oxidisation may have etched the sisal fibers and roughened their surfaces, thereby increasing the scatter of the strength data. Although observations of the SEM micrographs in Figure 10 support this proposal, quantitative measurements of surface roughness have not been obtained because of lack of appropriate techniques. By comparing $\sigma_0(s)$ values, it is shown that although silane treatments do not affect the fiber strength significantly, permanganate and DCP treatments do.

Figure 11a shows a SEM micrograph of a fractured untreated sisal fiber, whose major failure modes are pullout and fracture of the hollow microfibrils (that is, tearing of fiber cell walls). As discussed earlier, a sisal fiber has many microfibrils held together by a lignaceous material, and each microfibril has a composite structure consisting

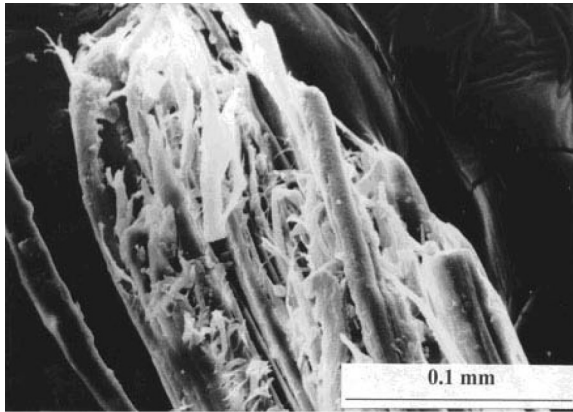


(a)

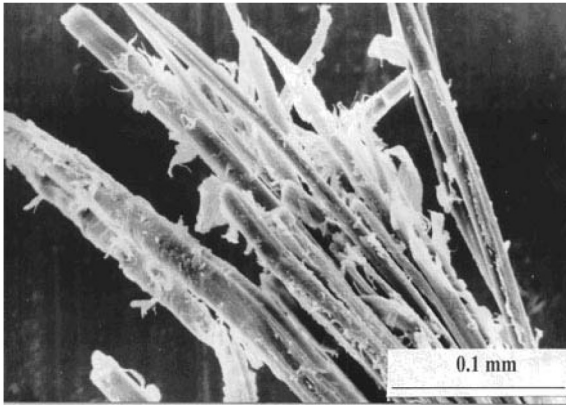


(b)

FIGURE 10 Surface feature of (a) permanganate-treated sisal fiber and (b) untreated sisal fiber.



(a)



(b)

FIGURE 11 Postfailure (after single-fiber tensile tests) SEM micrographs of (a) untreated sisal fiber and (b) permanganate-treated sisal fiber.

of oriented cellulose in a hemicellulose and lignin matrix. Thus, the strong fiber–matrix interfaces provide efficient load transfer to the fibers, leading to high tensile strength. Similar failure mechanisms occur in both silane-treated sisal fibers, and they explain why higher tensile strengths are obtained relative to permanganate and DCP-treated fibers.

In contrast, the main failure mechanism in the DCP- and permanganate-treated sisal fibers is the debonding or splitting of the failed microfibers seen in Figure 11b. DCP and permanganate are strong oxidants, and they can dissolve the lignin in the sisal, which

would act as a matrix for effective load transfer. Thus, after permanganate or DCP treatment, the bonding between the microfibers within a sisal fiber is reduced compared with the untreated and silane-treated sisal fibers. The poor interfacial properties of sisal fibers caused by permanganate and DCP treatments lead to a reduction of the tensile strength. (Uncoiling of the cell wall can also be seen in this micrograph.)

Sydenstricker, Mochnaz, and Amico [25] and Rong *et al.* [24] also investigated the effect of different surface treatments on sisal fiber strength. These include alkali, acrylamide, and silane treatments, amongst others. However, their results cannot be compared with those reported in this work because the treatment methods are not identical (even in the case of silane [24]).

3.2. Interfacial Properties Between Sisal Fiber and Three Different Matrices by Single Fiber Pullout Test

The IFSS of sisal/polyester was investigated by Sydenstricker, Mochnaz, and Amico [25]. They found that the IFSS improved from ~3 MPa for untreated fibers to 6–7 MPa for alkali- and acrylamide-treated sisal fibers. They thought that this was caused by better wettability of the resin on the fiber due to the chemical treatment, but there were no proof or discussions given. In the following, we present the IFSS results for sisal/vinyl ester, sisal/epoxy, and sisal/HDPE due to different fiber-treatment methods with possible interfacial mechanisms involved.

3.2.1. Interfacial Shear Strength (IFSS)

Sisal/vinyl ester. Figure 12 shows the load-displacement curves of single-fiber pullout tests for untreated, silane 1, silane 2, and permanganate- and DCP-treated sisal fibers embedded in vinyl ester resin. Two kinds of load-displacement curves are observed. The silane-treated and untreated sisal fibers show characteristics of stick-slips, but the other two types of treated fibers produced more stable pullout behaviors. These differences are later shown to be associated with the nature of the interface bonding. A linear relationship was observed for the maximum pullout load (P_{\max}) versus embedded fiber length (l) data for all fiber surface treatments. This means that the IFSS is a constant. IFSS can be calculated from

$$\text{IFSS} = \frac{P_{\max}}{2\pi al} \quad (3)$$

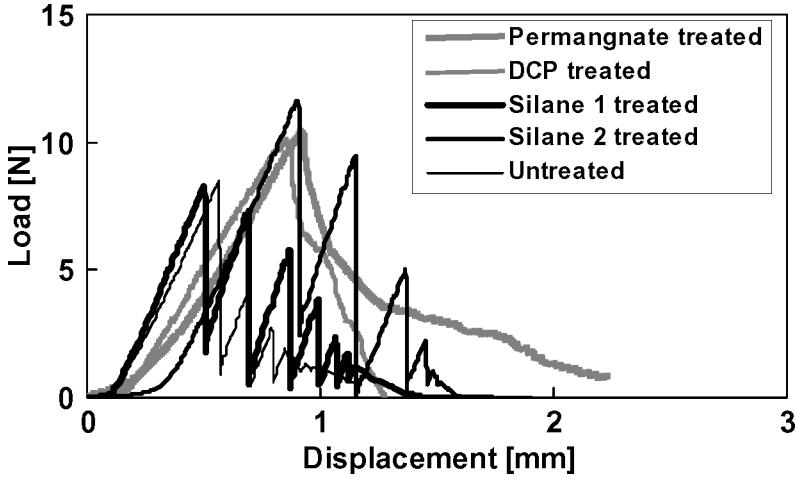


FIGURE 12 Load-displacement curves of single-fiber pullout tests for sisal/vinyl ester systems with different surface treatments.

where a is the fiber radius. Figure 13 shows the IFSS of the treated and untreated sisal fibers in a vinyl ester resin. The mean values and standard deviations are also shown in the histogram. It can be clearly seen that after fiber surface treatment with different chemical

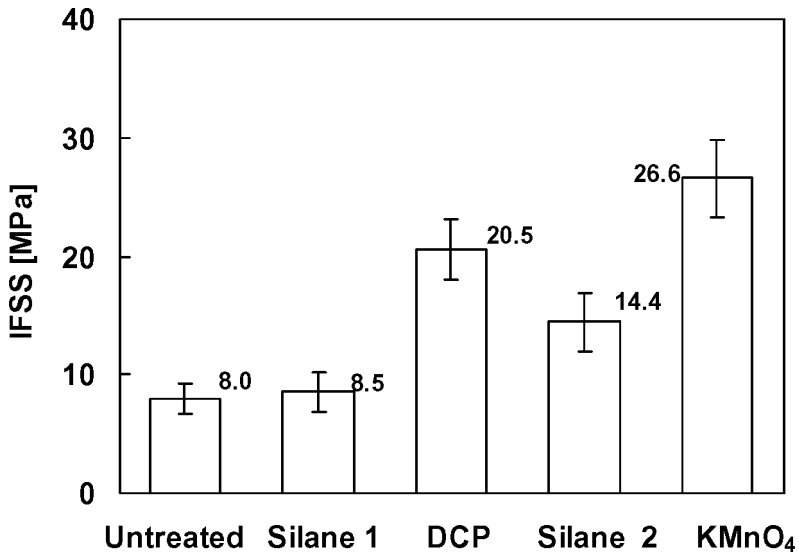


FIGURE 13 IFSS between sisal fiber and vinyl ester resin.

agents (except silane 1), the IFSS has been greatly improved. The KMnO_4 treatment shows the best effect and the IFSS between permanganate-treated sisal fiber and vinyl ester resin is almost three times that of the untreated fiber, followed by silane 2 and DCP treatments. For silane 1-treated sisal fibers, the IFSS is similar to that of the untreated-sisal-fiber-reinforced vinyl ester.

Though oxidization and chemical coupling can both improve the IFSS between sisal fiber and vinyl ester resin, the bonding mechanisms are quite different. The load-displacement curves of DCP- and KMnO_4 -treated sisal fibers are typical of a stable pullout process of a mainly mechanically bonded interface as described by Zhou *et al.* [30]. The rising portion of the load *versus* displacement curve is characteristic of elastic bonding at the fiber-matrix interface until the maximum load, at which time fiber frictional pullout commences. The oxidization of the permanganate- or DCP-treated sisal fiber makes its surface quite rough as a result of the etching effect. The dissolution of lignin may also allow ingress of the resin to the fiber. The nature of the bonding is mainly mechanical interlock with very little chemical bonding. So, the linear increase in load represents primarily the frictional shear stress transfer across the interface without debonding until the frictional resistance over the entire embedded fiber length is overcome. From SEM micrographs, it is seen that the surface of permanganate- (Figure 11a) and DCP-treated sisal fiber is relatively coarser than the untreated fiber (Figure 11b). Also, a KMnO_4 treated sisal fiber that is pulled out from vinyl ester shows a fair amount of resin residue on the fiber surface relative to an untreated pulled-out fiber. The decreasing portion of the load-displacement curve is self-explanatory as the fiber is progressively pulled out from the matrix.

Silane-treated and untreated sisal fibers show an unstable debonding process from their load-displacement curves during the single-fiber pullout tests (Figure 12). The initial debond leads immediately to complete debonding along the full fiber length. Figure 14 was taken from a sample instantaneously unloaded at maximum load during the pullout test. Complete interface debonding is evident. The load-displacement curve shows a monotonic increase in load until debonding is initiated, followed by a precipitous load drop, indicating complete debonding. There are also several stick-slips seen on the load-displacement curves during frictional sliding, possibly caused by the nonuniformity of the sisal fiber structure and diameter. The diameter of sisal fiber varies from 100 to 300 μm . From the study by Liu, Zhou, and Mai [31], the radial stress at the interface caused by the interfacial roughness can be determined by the material constants, such as Young's modulus and Poisson ratio of fiber and matrix, respectively, and asperity mismatch. The larger

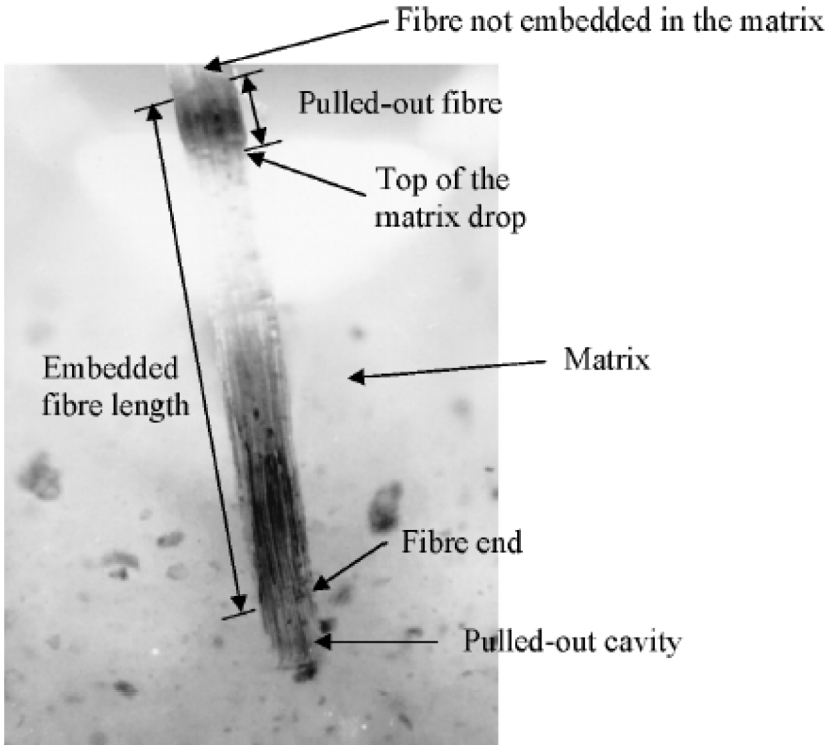
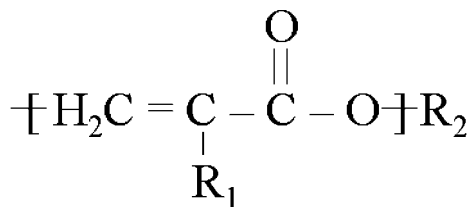


FIGURE 14 Complete interface debonding immediately after maximum load was applied during fiber pullout test for Silane 2 to treated sisal fiber.

the matrix modulus, the larger the radial stress. The elastic modulus of vinyl ester used in the present experiment is quite high (2.2 GPa) and is large enough to cause high asperity pressure between fiber and matrix. During fiber sliding, the geometric mismatch between fiber and matrix along its pullout length leads to the stick-slips.

When silane-treated sisal fibers were combined with the matrix, the long molecular chains of silane chemically bonded with the resin. Both silane 2 and vinyl ester have C=C groups (Figure 15). Therefore, addition polymerization could occur between vinyl ester and silane 2. Thus, the chemical coupling function is fulfilled for the fiber, matrix, and silane 2, and the IFSS is greatly improved as a result of the introduction of the chemical bonding between fiber and matrix. SEM-EDAX (Energy Dispersive X-ray Analysis) surface analysis shows the presence of Si atoms on the pulled-out silane 2-treated sisal fibers (Figure 16). It is further observed that there is substantially more matrix material



R₁: H or CH₃

R₂: Epoxy resin

FIGURE 15 Schematic of vinyl ester resin used in this work.

attached to the fiber surface compared with the untreated fiber. For silane 1-treated sisal fiber, the C=C functional group on the vinyl ester cannot react with the other functional group of silane 1 (*i.e.*, NH₂). Thus, chemical reaction between silane 1 and vinyl ester is not possible. Therefore, the IFSS of silane 1-treated sisal-fiber-reinforced vinyl ester cannot be improved and is similar to the IFSS of the untreated sisal fiber.

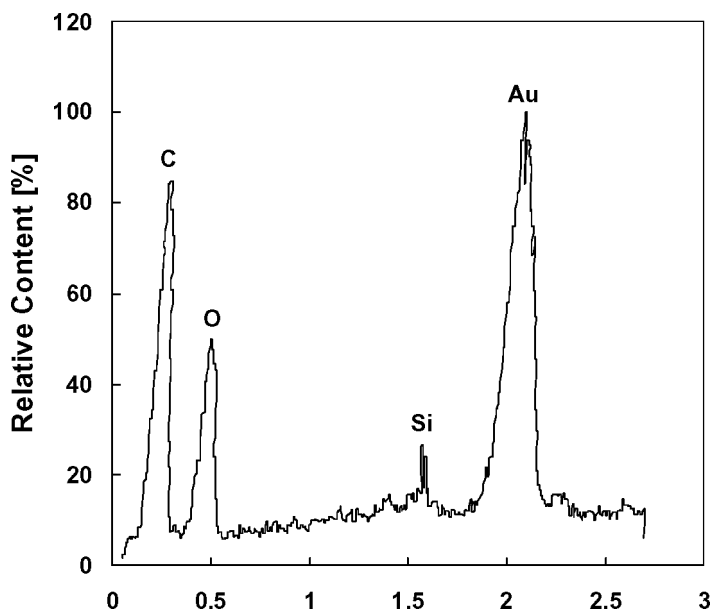


FIGURE 16 SEM surface detection of Si atoms on pulled out silane-treated sisal fibers (Au atoms were from gold coating for SEM specimens).

Sisal/epoxy. Interfacial properties of silane 2- and permanganate-treated, and untreated sisal-fiber-reinforced epoxy were studied in the same way as the sisal/vinyl ester single-fiber tests. Figure 17 shows IFSS results of treated and untreated sisal fibers in epoxy resin. The permanganate treatment improves the interfacial shear strength because of the mechanical bonding caused by the enhanced sisal fiber surface roughness and also penetration of epoxy to the fiber. Silane 2 has no effect on interface bonding, and the IFSS is similar to untreated fiber. Examination of the functional group of epoxy resin used in this work (Figure 18) shows that it cannot react with the functional group of silane 2 (*i.e.*, C=C). Thus, no chemical reactions can occur between them, and the coupling function of silane cannot be fulfilled. Thus, no improvement of interfacial properties between silane 2-treated sisal fiber and epoxy resin can be found.

Load-displacement curves of untreated and silane- and permanganate-treated sisal fibers during single-fiber pullout tests indicate two different failure mechanisms (Figure 19): stable debonding for permanganate-treated sisal-fiber-reinforced epoxy and unstable debonding followed by several stick-slips during frictional sliding of both untreated and silane-treated sisal fibers. The mechanisms of these debonding processes are the same as those of the composites with vinyl ester resin.

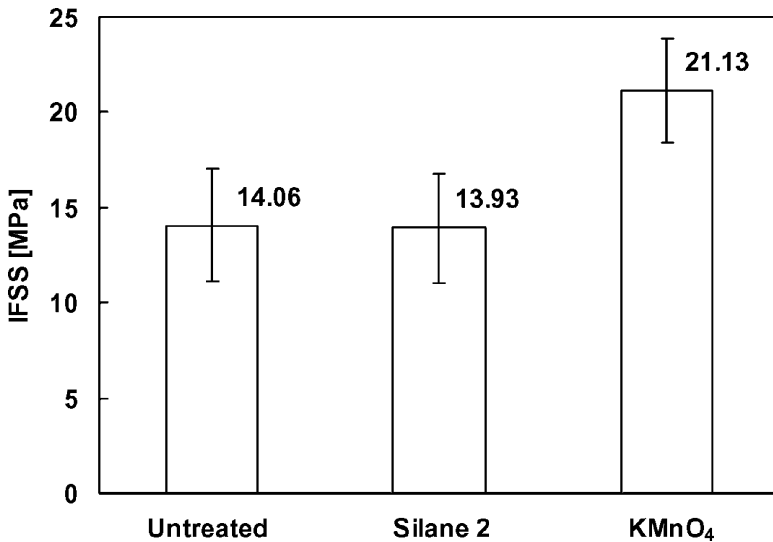


FIGURE 17 IFSS between treated and untreated sisal fiber and epoxy resin.

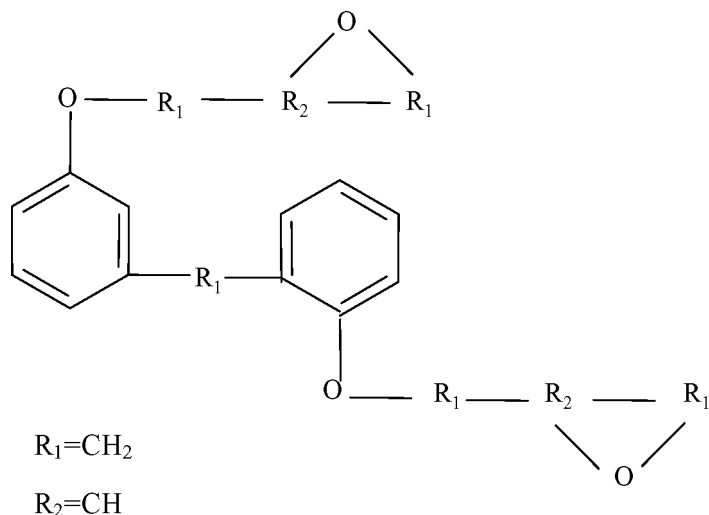


FIGURE 18 Schematic of EPON[®] 862 epoxy resin.

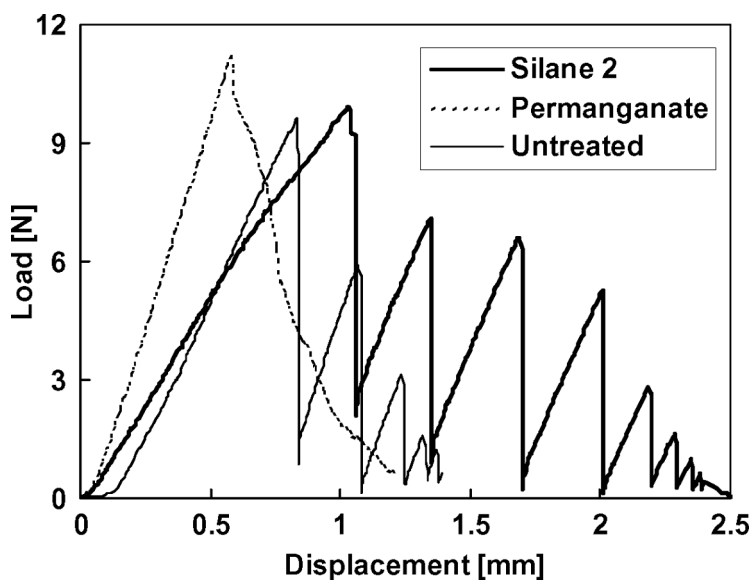


FIGURE 19 Load-displacement curves of treated and untreated sisal-fiber-reinforced epoxy resin during single-fiber pullout tests.

Sisal/HDPE. The load-displacement curves obtained for both treated and untreated sisal fibers with HDPE during single-fiber pull-out tests are shown in Figure 20. These curves show the characteristics of the stable debonding process for untreated and DCP- and KM_nO_4 -treated fibers, and unstable debonding for silane-treated fibers. The load-displacement curves of untreated and permanganate- and DCP-treated sisal fibers pulling out from the HDPE matrix are similar to those observed for permanganate- and DCP-treated sisal fibers from vinyl ester and epoxy resins, indicating a mechanical interlock between fiber and matrix. The load-displacement curve of silane-treated sisal fiber in HDPE is different from those of silane-treated sisal fibers in vinyl ester and epoxy resin during frictional sliding. There are no major multiple stick-slips, possibly because the radial clamping pressure on the fiber due to HDPE is much smaller, because the elastic modulus of HDPE is 1.1 GPa, which is about one-half and one-third of vinyl ester and epoxy, respectively.

Figure 21 shows that the IFSS of sisal fibers in the HDPE matrix can be improved considerably by appropriate fiber surface treatments. Permanganate and DCP can etch the sisal fiber surface and make it rougher, so that mechanical interlocking can be promoted between fiber and matrix. However, because only a very slight pressure was applied in hot-pressing, the penetration of HDPE into the sisal fiber

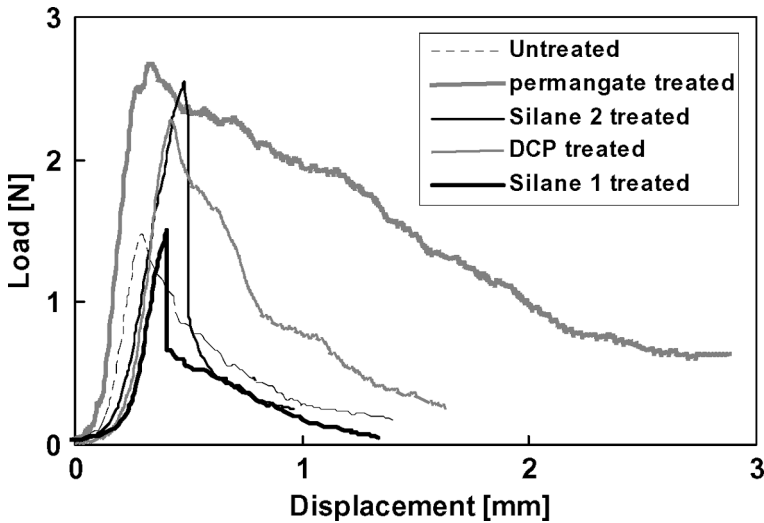


FIGURE 20 Load-displacement curves of single-fiber pullout tests for sisal/HDPE systems with different surface treatment.

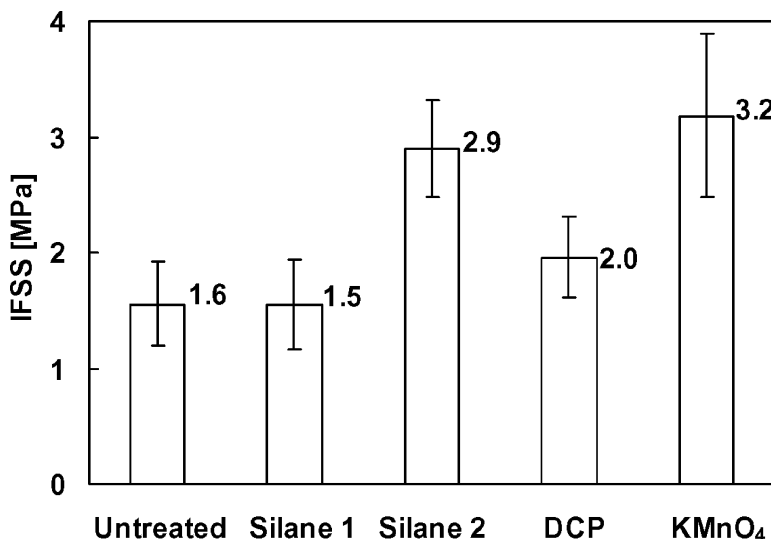


FIGURE 21 IFSS between sisal fiber and HDPE matrix.

would not be as effective as in both vinyl ester and epoxy resins, leading to lower IFSS values. (Compare data shown in Figure 21 with Figures 13 and 17.) Silane 2 has a carbon main chain, which could set up van der Waals bonds with the HDPE matrix because of their similar chemical structures. Though van der Waals bonds are not as strong as other primary bonds, they could still improve the bonding property between sisal fiber and HDPE matrix. In this context, it should be noted that HDPE is nonpolar and sisal is poorly polar, thus leading to generally weak bonding between them. Silane 1 does not have a carbon chain structure, so no chemical bonding can occur between HDPE and sisal fiber. Hence, IFSS between silane 1-treated sisal fiber and HDPE is similar to the untreated fiber. IFSS of treated and untreated sisal fibers with HDPE are ranked as follows: permanganate-treated sisal/HDPE > silane 2-treated sisal/HDPE > DCP-treated sisal/HDPE > untreated sisal/HDPE > silane 1-treated sisal/HDPE.

3.3. Interfacial Properties of the Composites made from Sisal Textile with Different Matrices by Short Beam Shear Test

3.3.1. Effect of Fiber Surface Treatment on Interlaminar Shear Strength (ILSS) of Sisal-Textile-Reinforced Vinyl Ester Resin

Figure 22 shows the ILSS of sisal-textile-reinforced vinyl ester resin as affected by different fiber surface treatments. Both silane 2 and

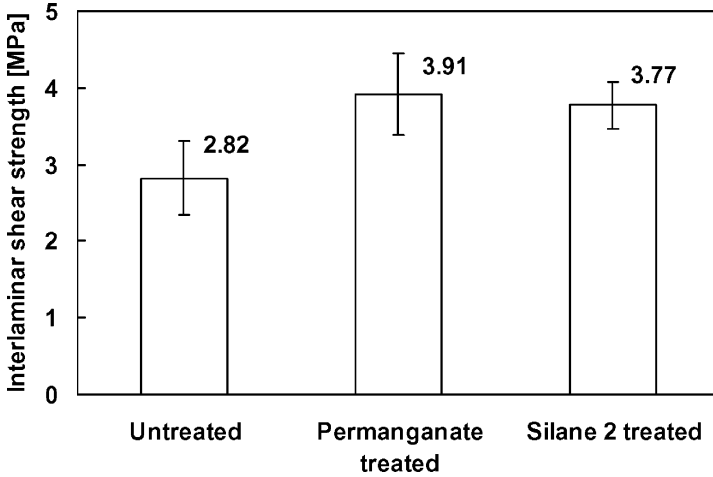


FIGURE 22 Interlaminar shear strength (ILSS) of sisal-textile-reinforced vinyl ester.

permanganate improve the ILSS from 2.82 MPa of untreated fibers to 3.77–3.91 MPa after surface treatment. These results are consistent with the IFSS data in Section 3.2.1, because permanganate treatment enhances mechanical interlocking and silane 2 improves the chemical bonding between fiber and matrix.

By examining the sisal-textile-reinforced vinyl ester composite after the SBS tests (Figure 23), we can see severe delamination is the major failure mode, which occurs mainly along the fiber–matrix interface. There is less delamination in the silane 2- and permanganate-treated sisal textile/vinyl ester composites than the untreated sisal textile/vinyl ester composite. Hence, higher ILSSs are obtained (see Figure 22).

3.3.2. Effect of Fiber Surface Treatment on ILSS of Sisal-Textile-Reinforced Epoxy Resin

Figure 24 shows the ILSS of treated and untreated sisal textile/epoxy composites. Permanganate increases the SBS strength of untreated sisal textile/epoxy from 4.76 MPa to 6.73 MPa, but silane 2 treatment has no effect on the ILSS of the composite. Permanganate treatment enhances the fiber surface roughness and, hence, the contact area between fiber and matrix. Thus, a higher ILSS is caused by better interface bonding. In contrast, silane 2 treatment cannot improve the interfacial bonding properties between sisal fiber and epoxy (see Figure 17). Hence, the ILSS is also similar to the untreated sisal textile/epoxy composite.

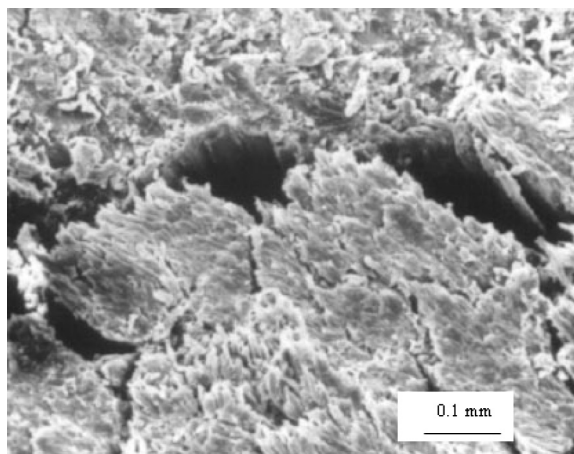


FIGURE 23 Severe delamination of untreated sisal-textile-reinforced vinyl ester after the short beam shear tests.

By comparing the micrographs for an untreated and a permanganate-treated sisal fiber bundle of the specimen after SBS testing, it can be observed that a relatively clean surface is seen on the untreated sisal bundle, indicating poor interfacial bonding between sisal fiber and epoxy. However, a large amount of epoxy is observed attached on the permanganate-treated sisal fibers. This indicates that permanganate treatment leads to better interfacial bonding between sisal fiber and epoxy resin. These results qualitatively support the ILSS data shown in Figure 24.

4. CONCLUSIONS

Sisal fiber can be regarded as a cellulose-reinforced lignin composite material. Unlike manmade fibers, the structure and properties of sisal fibers are nonuniform. The Weibull method is useful for studying the tensile properties of treated and untreated sisal fibers. Permanganate- and DCP-treated sisal fibers have lower tensile strength and larger scatter of strength data compared with untreated and silane-treated sisal fibers. Tensile fracture of sisal fibers involves microfiber interface debonding, microfiber pullout, and breakage. Like many composite materials, good interfacial adhesion leads to high tensile strength. Thus, permanganate and DCP treatments cause poor microfiber interfaces and lead to reductions of tensile strength.

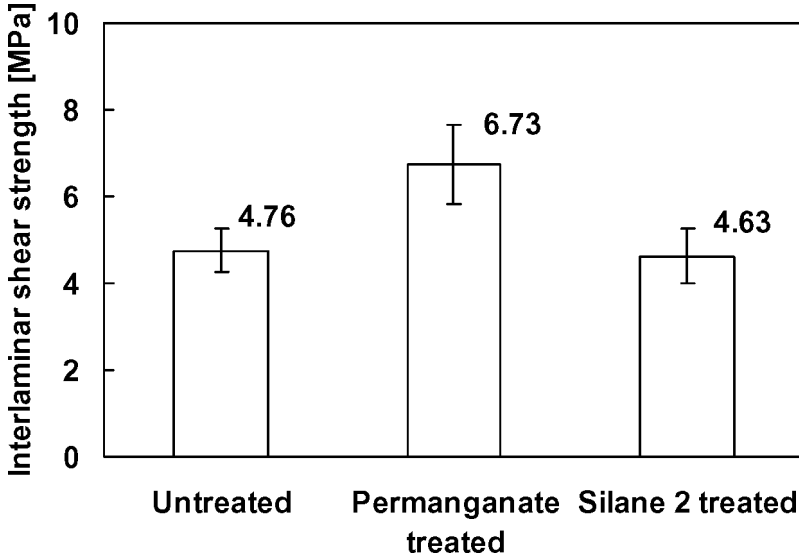


FIGURE 24 Interlaminar shear strength (ILSS) of sisal-textile-reinforced epoxy resin.

The interfaces between sisal fibers and polymer matrices (vinyl ester, epoxy, and HDPE) are very poor because of the hydrophilic nature of cellulose and the absence of functional groups on the fiber surface. Fiber surface treatments are useful for modification of interfacial properties between sisal fiber and vinyl ester, epoxy, or HDPE. Different matrices require different fiber surface treatment methods. Single-fiber pullout tests and SEM observations show that KMnO_4 and DCP roughen the fiber surface and introduce mechanical interlocking with the matrix. This is identified as the major contribution to the interface bonding between permanganate- and DCP-treated sisal-fiber-reinforced polymers.

Gamma-methacryloxypropyltrimethoxy silane (silane 2) reacts with sisal fiber, vinyl ester, and HDPE matrices. Thus, IFSS can be substantially improved. However, silane 2 does not react with epoxy, which results in IFSS similar to the untreated fibers. 3-Aminopropyltriethoxy silane (silane 1) can only react with the sisal fiber but not the polymers, so IFSS is almost the same as that of the untreated sisal fiber composite.

Two kinds of debonding processes of treated and untreated sisal fibers in vinyl ester, epoxy, and HDPE matrices were noted. Permanganate- and DCP-treated sisal fibers showed stable debonding,

whereas untreated and silane-treated sisal fibers displayed unstable debonding in all three matrices. Multiple stick–slips were observed in frictional sliding of silane-treated fibers in both vinyl ester and epoxy resins but not in HDPE.

Fiber surface treatments can improve the apparent ILSS of sisal-textile-reinforced vinyl ester and epoxy resins. Delamination damage at the sisal fiber–matrix resin interface is the major failure mode. Fewer delaminations between sisal fiber and matrix were observed in treated sisal textile than untreated sisal textile composites after the SBS tests, which are due to the improved interfacial bonding in the former.

REFERENCES

- [1] Ganan, P. and Mondragon I., *J. Compos. Mater.* **39**, 633–646 (2005).
- [2] Belgacem, M. N. and Gandini, A., *Compos. Interface.* **12**, 41–77 (2005).
- [3] Sreekala, M. S. and Thomas, S., *Compos. Sci. Technol.* **63**, 861–869 (2003).
- [4] Mohanty, A. K., Misra, M., and Drzal, L. T., *Natural Fibers, Biopolymers, and Biocomposites* (CRC Press, Boca Raton, FL, 2005).
- [5] Baillie, C., *Green Composites: Polymer Composites and the Environment* (Woodhead Publishing Limited, Cambridge, Cambridge, UK, 2004).
- [6] Franck, R. R., *Bast and Other Plant Fibers* (Woodhead Publishing Limited, Cambridge, Cambridge, UK, 2005).
- [7] Chand, N., Sood, S., Rohatgi, P. K., and Satyanarayana, K. G., *J. Sci. Ind. Res. India* **43**, 489–499 (1984).
- [8] Holmer, S. J., Vahan, A., Adriana, M. N., and Lia, P., *Constr. Build. Mater.* **13**, 433–438 (1999).
- [9] Singh, B., Gupta, M., and Verma, A., *Constr. Build. Mater.* **9**, 39–44 (1995).
- [10] Van de Velde, K. and Kiekens, P., *J. Thermoplast. Compos.* **16**, 413–431 (2003).
- [11] Dahlke, B., Larbig, H., Scherzer, H. D., and Poltrock, R., *J. Cell. Plast.* **34**, 361–368 (1998).
- [12] Sherman, L. M., *Plastics Technology* **10**, 62–68 (1999).
- [13] Li, H., Pawel, Z., and Per, F., *Polym. Composite.* **8**, 199–207 (1987).
- [14] Zhou, L. M., Kim, J. K., and Mai, Y.-W., *Compos. Sci. Technol.* **45**, 153–160 (1992).
- [15] Zhou, L. M., Kim, J. K., and Mai, Y.-W., *Compos. Sci. Technol.* **48**, 227–236 (1993).
- [16] Kim, J. K. and Mai, Y.-W., *Engineered Interfaces in Fiber Reinforced Composites* (Elsevier Science Ltd., Oxford, UK, 1998), p. 401.
- [17] Li, Y., Mai, Y.-W., and Ye, L., *Compos. Interface.* **12**, 141–163 (2005).
- [18] Ganan, P., Garbizu, S., Llano-Ponte, R., and Mondragon, L., *Polym. Composite.* **26**, 121–127 (2005).
- [19] Nair, K. C. M. and Thomas, S., *Polym. Composite.* **24**, 332–343 (2003).
- [20] Singh, B., Gupta, M., and Verma, A., *Polym. Composite.* **17**, 910–918 (1996).
- [21] Joseph, K. and Thomas, S., *Polymer.* **37**, 5139–5149 (1996).
- [22] Kim, J. K., Lu, S., and Mai, Y.-W., *J. Mater. Sci.* **29**, 554–561 (1994).
- [23] Kim, J. K., Zhou, L. M., and Mai, Y.-W., *J. Mater. Sci.* **28**, 3923–3930 (1993).
- [24] Rong, M. Z., Zhang, M. Q., Liu, Y., Yang, G. C., and Zeng, H. M., *Compos. Sci. Technol.* **61**, 1437–1447 (2001).

- [25] Sydenstricker, T. H. D., Mochnaz, S., and Amico, S. C., *Polym. Test.* **22**, 375–380 (2003).
- [26] Ji, X., Dai, Y., Zheng, B. L., Ye, L., and Mai, Y.-W., *Composite Interfaces* **10**, 567–580 (2003).
- [27] Bisanda, E. T. N. and Ansell, M. P., *J. Mater. Sci.* **27**, 1690–1700 (1992).
- [28] Watson, A. S. and Smith, R. L., *J. Mater. Sci.* **20**, 3260–3270 (1985).
- [29] Sybrand, Z., *J. Test. Eval.* **17**, 292–298 (1989).
- [30] Zhou, L. M., Mai, Y.-W., Ye, L., and Kim, J. K., *Key. Eng. Mater.* **104–107**, 549–600 (1995).
- [31] Liu, H. Y., Zhou, L. M., and Mai, Y.-W., *Philos. Mag. A.* **70**, 359–372 (1994).